

Published in final edited form as:

*Cancer Prev Res (Phila)*. 2011 December ; 4(12): 2122–2130. doi:10.1158/1940-6207.CAPR-11-0376.

## Bitter melon extract impairs prostate cancer cell cycle progression and delays prostatic intraepithelial neoplasia in TRAMP model

Peng Ru<sup>1</sup>, Robert Steele<sup>1</sup>, Pratibha V. Nerurkar<sup>3</sup>, Nancy Phillips<sup>1</sup>, and Ratna Ray<sup>1,2,\*</sup>

<sup>1</sup>Department of Pathology, Saint Louis University, St. Louis, Missouri

<sup>2</sup>Department of Internal Medicine, Saint Louis University, St. Louis, Missouri

<sup>3</sup>Laboratory of Metabolic Disorders and Alternative Medicine, Department of Molecular Biosciences and Bioengineering, College of Tropical Agriculture and Human Resources, University of Hawaii, Honolulu, Hawaii

### Abstract

Prostate cancer remains the second leading cause of cancer deaths among American men. Earlier diagnosis increases survival rate in patients. However, treatments for advanced disease are limited to hormone ablation techniques and palliative care. Thus, new methods of treatment and prevention are necessary for inhibiting disease progression to a hormone refractory state. One of the approaches to control prostate cancer is prevention through diet, which inhibits one or more neoplastic events and reduces the cancer risk. For centuries, Ayurveda has recommended the use of bitter melon (*Momordica charantia*) as a functional food to prevent and treat human health related issues. In this study, we have initially used human prostate cancer cells, PC3 and LNCaP, as an *in vitro* model to assess the efficacy of bitter melon extract (BME) as an anti-cancer agent. We observed that prostate cancer cells treated with BME accumulate during the S phase of the cell cycle, and modulate cyclin D1, cyclin E and p21 expression. Treatment of prostate cancer cells with BME enhanced Bax expression, and induced poly(ADP-ribose) polymerase cleavage. Oral gavage of BME, as a dietary compound, delayed the progression to high grade prostatic intraepithelial neoplasia (PIN) in TRAMP (transgenic adenocarcinoma of mouse prostate) mice (31%). Prostate tissue from BME-fed mice displayed ~51% reduction of PCNA expression. Together, our results suggest for the first time that oral administration of BME inhibits prostate cancer progression in TRAMP mice by interfering cell cycle progression and proliferation.

### Keywords

BME; prostate cancer; cyclins; apoptosis; TRAMP model

### INTRODUCTION

Prostate cancer is the most commonly diagnosed cancer in men and one of the leading causes of cancer death in the USA (1). Although prostate cancer is frequently curable in its early stage by surgical or radiation ablation, many patients present locally advanced or metastatic disease for which there are currently no curative treatment options (2, 3). Therefore, more effective therapies that can cure localized tumors and prevent their

\*Requests for reprints: Ratna B. Ray, Department of Pathology, Saint Louis University, 1100 South Grand Boulevard, St. Louis, MO 63104. Phone: 314-977-7822; Fax: 314-771-3816; rayrb@slu.edu.

metastasis are urgently needed. Cancer cells acquire resistance to apoptosis by overexpression of antiapoptotic proteins and/or by the downregulation or mutation of proapoptotic proteins. The intervention of multistage cancer by modulating intracellular signaling pathways may provide a molecular basis for chemoprevention with a wide variety of dietary phytochemicals (4). Therefore, an ideal approach to inhibit the progression of cancer is to induce cell cycle arrest or apoptosis using dietary chemopreventive compounds.

*Momordica charantia*, also known as bitter melon, balsam pear, or karela, is widely cultivated in Asia, Africa, and South America and extensively used in folk medicines as a remedy for diabetes, specifically in India, China, and Central America (5). Animal studies have employed either fresh bitter melon extract (BME) or crude organic fractions to evaluate its beneficial effects on glucose metabolism and on plasma and hepatic lipids (6–11).

The anti-tumor activity of crude BME in murine lymphoma was reported earlier (12), although the mechanisms are poorly understood. *Momordica* protein of 30 kDa (MAP 30), isolated from bitter melon seeds, displayed anti-tumor activity in breast cancer model (13). The chemical modification of BME RIP significantly reduced its *in vivo* immunogenicity, but retained its anti-proliferative activity as measured by DNA fragmentation and caspase-3 activation (14). The bitter melon seed extracts displayed anticancer activity in a rat colonic aberrant crypt foci model and a mouse mammary tumor model (15, 16). However, the acetone extract of bitter melon seed, which is probably rich in  $\alpha$ -eleostearic acid, did not suppress the colon cancer growth in xenograft model (17). Therefore, more work will be necessary to understand the *in vivo* activity of bitter melon.

To our knowledge, this is the first study to demonstrate that BME prevents prostate cancer progression in TRAMP (transgenic adenocarcinoma of the mouse prostate) mice model. Mechanistic studies further indicate that treatment of prostate cancer cells with BME accumulates cells at the S phase of the cell cycle, and induces cell cycle arrest and apoptosis.

## Materials and Methods

### Cells and preparation of bitter melon extract (BME)

Prostate cancer cells (PC3 and LNCaP) (obtained from ATCC), were maintained in DMEM and RPMI with 10% FCS, respectively. Primary human prostate epithelial cells were obtained from Lonza, and maintained for short time in specified media. Cell lines have not been independently authenticated. BME was prepared from the Chinese variety of young bitter melons (raw and green) as discussed previously (10). Briefly, BME was extracted using a household juicer and centrifuged at  $560 \times g$  at 4°C for 30 min, freeze dried at -45°C for 72 h and stored at -80°C until used for feeding studies. We prepared a stock of 0.1g/ml in water, aliquoted, used 2% (vol/vol) for *in vitro* cell culture work and 100  $\mu$ l/mouse for oral gavage.

### FACS analysis

PC3 and LNCaP cells were treated with BME for 24 h. Cells were trypsinized and fixed in ice-cold 70% ethanol overnight at 4°C. Cells were washed, stained with propidium iodide for overnight and subjected to FACS analysis on a FACScan flow cytometer (BD PharMingen) as described previously (18, 19). Data were analyzed using the CellQuest and ModFit software.

### Western blot analysis

Prostate cancer cells were untreated or treated with BME at different time points, and cell lysates were prepared in 2 $\times$  SDS sample buffer. Cell lysates were analyzed for Western blot

analysis using poly(ADP-ribose) polymerase (PARP), caspase-3, caspase -7, cyclin D1, cyclin E, p21, phospho-MEK1/2, total MEK1/2, phospho-p38, total p38, phospho-ERK1/2, total ERK1/2, PCNA and Bax antibodies (Santa Cruz Biotechnology, Santa Cruz, CA or Cell Signaling, Danvers, MA), followed by enhanced chemiluminescence (Amersham Biosciences, Piscataway, NJ). Blots were reprobated with actin to compare protein load in each lane.

### Animals and BME treatment

We chose TRAMP mice for our studies because TRAMP males develop spontaneous multistage prostate carcinogenesis that exhibits both histological and molecular features recapitulating many salient aspects of human prostate cancer (20, 21). Further, TRAMP model has been used successfully to test chemopreventive efficacy of several natural agents (22–25). Tg(TRAMP)8247 Ng mice) male mice (~5 weeks old) were purchased from the Jackson Laboratory and divided into two groups (10 mice in each group) randomly to examine the effects of BME treatment on prostatic intraepithelial neoplasia (PIN) in TRAMP mice. Mice at 6 weeks received 0.1 mL water by oral gavage (control group) and 0.1 mL BME by oral gavage (experimental group), 5 days/wk for a period of 15 weeks. The mice were sacrificed 24 h after the last administration of the water or BME by CO<sub>2</sub> inhalation. A portion of the prostate/tumor tissue was placed in 10% neutral buffered formalin and paraffin-embedded. The other portion of the dorsolateral prostate was snap-frozen and stored at –80°C. During the study, animals were permitted free access to food and drinking water, and the animals were monitored daily for their general health. All animal treatments were according to the protocol approved by the Institutional Animal Care and Use Committee, and NIH guide lines.

### Pathological evaluation and scoring of tumor stage

Randomly selected fields (10–20) of H&E stained sections (5-μm thick) of the dorsolateral prostate (DLP) from individual mice of both control and BME-fed groups were independently scored (blinded) by two researchers for incidence of prostate cancer. The percentage of area corresponding to each pathological stage was also counted. Pathological grading was performed based on Shappell et al. (26).

### Immunohistochemical analysis

The paraffin-embedded sections (5-μm thick) were deparaffinized and stained using antibody against proliferating cell nuclear antigen (PCNA) or SV40 T-antigen followed by 3,3'-diaminobenzidine staining. Ten fields of DLP (each animal) from the control and BME-fed groups were scored by two researchers, and the relative percentage of PCNA expression cells was calculated.

### Statistical analysis

All statistical analyses were carried out with STATISTICAL ANALYSIS SYSTEM software (GraphPad Prism 4.03), and P values less than 0.05 were considered significant.

## RESULTS

### BME treatment induces S phase arrest in prostate cancer cells and modulates cell cycle regulators

We have initially treated prostate cancer cells with BME at different time points, and cell viability was determined by trypan blue exclusion. Prostate cancer cells died (>90%) within 96 h of BME treatment, whereas primary prostate epithelial cells exhibited very little effects. We selected two prostate cancer cell lines, PC3 (androgen receptor -negative and mutant

p53) and LNCaP (androgen receptor-positive and wild type p53) for subsequent studies. To understand the mechanism of BME mediated proliferation inhibition, we examined the effect of BME on the cell cycle by FACS as described previously (18, 19). Cell populations in the G<sub>0</sub>-G<sub>1</sub> and S phases were 51% and 35% in control PC3 cells. However, after 24 h incubation with BME, the S population was noticeably enhanced to 45%, whereas the G<sub>0</sub>-G<sub>1</sub> population was decreased to 35% (Fig. 1A). We did not observe a significant change in the proportions of cells in G<sub>2</sub>/M phase. Similarly, BME treatment in LNCaP cells also displayed enhanced S phase, 24% vs. 12% in control untreated cells (Fig. 1B). This result suggests that BME treatment on prostate cancer cells induces S-phase arrest.

To identify cell cycle regulatory molecules, we examined the expression of cyclins and cyclin-dependent kinase (CDK) inhibitors. Cells were treated with BME for 48 and 72 h, and cell lysates were prepared for Western blot analysis. Our results suggested that the treatment of BME led to a significant downregulation of cyclin D1 and cyclin E in prostate cancer cell lines (Fig. 2A). We have also observed a significant increase of p21 protein in both the prostate cancer cell lines, suggesting an S phase arrest (Fig. 2B). Interestingly, the expression levels of p27 protein remained similar in BME treated PC3 and LNCaP cells as compared to untreated cells (Fig. 2B). Together these results suggested that BME treatment in prostate cancer cells strongly modulates cyclins and inhibits their normal regulation of cell cycle progression.

### **BME treatment activates p38MAPK and ERK1/2**

To further determine molecular pathways, we examined the activation of p38MAPK and ERK1/2, which are important upstream regulators of p21 (27, 28). Activation of p38MAPK and ERK1/2 are also correlated with the promotion of cell cycle arrest in prostate cancer (29, 30). Western blot analysis revealed that phospho-p38, the activate form of p38MAPK, was significantly induced following BME treatment in both PC3 and LNCaP cell lines (Fig. 3A). Next, activation of ERK1/2 was examined. Prostate cancer cells treated with BME displayed upregulation of phospho-ERK1/2 expression (Fig. 3B). We further examined the status of MEK1/2, an upstream regulator of ERK1/2. Activation of MEK1/2 was observed in BME-treated cells as compared to control (Fig. 3C). Together, these results suggested that BME treatment in prostate cancer cells activates MEK-ERK or p38MAPK signaling pathway.

### **BME treatment induces apoptosis *in vitro***

Cell cycle arrest was correlated with apoptosis (31). Since we observed cell cycle arrest, and ERK/p38 activation, we next examined whether BME treatment in prostate cancer cells induces apoptosis. Cleavage of the DNA repair enzyme poly (ADP-ribose) polymerase (PARP) from a 116 kD protein to a signature peptide of 86 kD fragment is associated with a variety of apoptotic responses. PARP is a nuclear protein and a downstream substrate of activated caspase-3/7. Prostate cancer cells treated with BME displayed a cleaved 86 kD signature peptide (Fig. 4A). We observed an induction of cleaved caspase-3/7 and 9 in prostate cancer cells treated with BME (Figs. 4B and 4C). Mitochondria play a pivotal role in cell homeostasis, and the mitochondria-pathway is tightly regulated by the Bcl-2 family proteins. To better understand the anti-cancer effect of BME treatment including growth inhibitory and pro-apoptosis effects, we next tested whether BME treatment induces the expression of pro-apoptosis markers in prostate cancer cells. Western blot analysis indicated that Bax was induced by BME treatment in both PC3 and LNCaP cell lines (Fig. 4D). These results showed that BME treatment in prostate cancer cells induces apoptosis.

## Oral administration of BME inhibited prostate cancer progression in TRAMP mice

The TRAMP mouse model is one of the popular mouse models for prostate cancer chemoprevention studies (22–25). These male mice develop spontaneous multistage prostate carcinogenesis that exhibits both histological and molecular features recapitulating many salient aspects of human prostate cancer. The transgene construct in these mice is a PB-Tag gene consisting of the minimal –426/+28 bp regulatory sequence of the rat probasin promoter directing prostate-specific epithelial expression of the SV40 T-antigen gene introduced into the C57BL/6 mouse (32). TRAMP males characteristically express the PB-Tag transgene by 8 weeks of age and display prostatic intraepithelial neoplasia (PIN) by 10–12 weeks of age (20). TRAMP (Tg(TRAMP)8247 Ng mice) male mice (5 weeks old) were purchased from the Jackson Laboratory and divided into two groups (10 mice in each group) randomly to examine the effects of BME treatment on prostate cancer development in TRAMP mice. The experimental group was gavaged BME (0.1 g/ml) 5 days a week, and control group were similarly fed with water. After 15 weeks of treatment with BME or water, TRAMP mice were sacrificed, prostates glands were removed, and formalin-fixed for immunohistochemistry analysis. The body weights of the control and BME-fed mice did not differ significantly throughout the experimental protocol. The mice were monitored everyday for signs of stress throughout the experimental period. At the time of sacrifice, all animals were examined for gross pathology, and there was no evidence of global edema, abnormal organ size or appearance in non-target organs. A significant weight difference of the prostate (70%,  $p<0.013$ ) was observed between control and experimental groups.

Histopathological analysis of the prostate displayed less aggressiveness in the BME-fed group (Fig. 5). H&E-stained sections of prostate glands were microscopically examined and classified based on Shappell et al. (26): (a) low-grade PIN having foci with two or more layers of atypical cells with elongated hyperchromatic nuclei and intact gland profiles, and (b) high-grade PIN having increased epithelial stratification, foci of atypical cells fill or almost fill the lumen of the ducts, enlarged diameter of glands, distorted duct profiles, increase in nuclear pleomorphism, hyperchromatic nuclei, and cribriform structures. We randomly selected 10 areas of each TRAMP mouse prostate section and scored the incidence of normal, low-grade PIN and high-grade PIN of prostate glands. The incidence of normal gland on the prostate section from BME-fed group was 64% significantly higher than observed in control group (23%,  $p<0.0002$ ). The incidence of low-grade PIN was similar from both groups. But the incidence of high-grade PIN from BME-fed group was 47% significantly lower than 78% from control group (Fig. 5A). We have observed ~21% area of prostate gland was histologically normal in BME-fed group as compared with ~12% normal glands in the control group (Fig. 5B). The area covered by low grade PIN lesions in BME-fed group was 41% more than that in the positive control group (29%), and high grade PIN in BME-fed group was 38% than that in the positive control group (59%). We did not observe invasive cancer, and very rarely the well differentiated stages were observed. A representative H&E staining in sections of DLP from control and BME fed mice are shown in Fig. 5C. We did not observe a difference in SV40 T-antigen expression in control and BME-fed mice prostate tissues (Fig. 5D). Our results demonstrated that control group displayed more high-grade PIN, whereas BME-fed group displayed low-grade PIN, suggesting that BME treatment significantly delayed the progression of PIN in TRAMP mice.

## BME feeding inhibits prostate cancer cell proliferation

To assess the *in vivo* effect of BME feeding on the proliferation index in the dorsolateral prostate, tissue samples from TRAMP mice were analyzed by PCNA immunostaining. A representative immunostaining slides displayed significant decrease in PCNA-positive cells in BME-fed group as compared to the control group (Fig. 6A). Quantitative microscopic



examination of PCNA-stained sections showed that PCNA-positive cells in BME-fed group were 49% as compared to control group (Fig. 6B). Western blot analysis of PCNA was further confirmed that PCNA expression was indeed inhibited in BME-fed mice as compared to control mice (Fig. 6C). We have also observed PARP cleavage (as observed decreased expression of full-length PARP) in BME-fed mice as compared to control TRAMP mice prostate tissues (Fig. 6D). Together these results suggested that BME treatment in TRAMP mice strongly reduces PCNA expression that may prevent prostate tumor progression in TRAMP mice.

## DISCUSSION

The novel findings in this study are that (i) BME treatment in prostate cancer cells induces cell cycle arrest and eventually cell death, (ii) BME feeding in TRAMP mice inhibits prostate tumor progression without any toxicity, and (iii) the chemopreventive efficacy of BME is accompanied by delays of tumor progression at high grade PIN, and a decrease in cell proliferation. The potential molecular mechanisms of BME mediated inhibition of prostate cancer growth are a decrease in expression of critical cell cycle regulatory proteins cyclin D1 and cyclin E as well as a block in S phase, with a concomitant increase in p21 protein level. This is the first report to our knowledge describing the mechanism of BME mediated prostate cancer growth inhibition.

Uncontrolled cell growth and resistance to apoptosis are major defects in neoplasia. Development of approaches that induce the apoptotic machinery within cancer cells could be effective against their proliferation and invasive potential (33). A number of agents such as  $\gamma$ -irradiation, immunotherapy, and chemotherapy induce apoptosis in tumor cells as the primary mode of action for most anticancer therapies. Impairment of this pathway is implicated in treatment resistance (34). In fact, many chemopreventive agents of natural origin have shown promising anticancer properties by induction of the apoptotic pathway in transformed or tumor cells (4, 35). In the last few decades, considerable progress has been made in this direction leading to identification of many cancer chemopreventive agents, one of them being bitter melon, which has shown anticancer effects in other cancer cell types (12–17, 19, 36). Over the years, there has been a worldwide interest in BME as a dietary supplement because of its various health benefits, including lowering diabetes and lipidemia (9, 11). In a different study, we have shown that BME is well tolerated, and has been termed as relatively safe in acute, subchronic, and chronic doses in animals (9).

The CDK inhibitors (p21, p27 and p57) causes cell cycle arrest and inhibit the growth of cancer cells (37–40). Our *in vitro* results indicated that cyclin D1 and cyclin E were down-regulated in BME treated prostate cancer cells, and cyclin A was decreased in BME treated PC3 cells (data not shown), whereas the CDK inhibitor p21 was up-regulated, suggesting that BME inhibited prostate cell growth through the arrest of cell cycle and inhibition of proliferation. Interestingly, BME treatment in prostate cancer cells did not alter survivin expression as observed in breast cancer cells (19). We also observed the activation of p38 and ERK1/2 in prostate cancer cells treated with BME. p38MAPK and ERK1/2 are reported to be the upstream regulator of p21 (37) and involved in p21 dependent cell cycle arrest (41). In prostate cancer, activation of p38 and ERK1/2 are also reported to promote apoptosis (42, 43). MEK1/2 is the upstream regulator of ERK1/2, which is also involved in the induction of apoptosis in prostate cancer (44). Our result indicated that BME treatment activates MEK-ERK and p38MAPK pathway, thereby inducing cell cycle arrest and apoptosis.

In humans, prostate cancer progression is a multistage process involving an onset as a small carcinoma of low histologic grade, which progresses slowly towards metastatic lesions of

higher grade disease. In TRAMP model, prostate cancer development closely mimics this human prostate cancer progression (20, 32). We have shown that BME-fed mice displayed lower incidence of high-grade as compared to control mice. This suggests that BME feeding for 15 weeks starting from the 6th week of age causes inhibition or delay of the tumor progression at the neoplastic stage. We also found that oral administration of BME causes a statistically significant decrease in cell proliferation in the dorsolateral prostate of TRAMP mice, as evidenced by reduced expression of PCNA, and PARP cleavage. Therefore, the antitumor progression effect of BME in TRAMP mice could most likely be mediated, at least in part, via its effect on Cdk-cyclin-Cdk inhibitor axis.

In conclusion, the results of the present study indicates, for the first time, that BME modulates cell cycle regulatory molecules thereby causing cell cycle arrest and eventually apoptosis in prostate cancer cells. Oral administration of BME significantly inhibits prostate cancer progression in TRAMP mice without any adverse health effects or reducing T-antigen expression. Together, these results suggest that BME modulates several signal transduction pathways which additively or synergistically restrict prostate cancer growth, and can be utilized as dietary supplement for prevention of prostate cancer.

## Acknowledgments

We thank Dr. Cheri West, Frank Speck, Frank Strebeck and Anna Knobeloch for helping BME feeding to TRAMP mice and prostate tissues isolation, and Peter Humphrey for helpful discussion. This work was supported by research grant R21CA137424 from the National Institutes of Health.

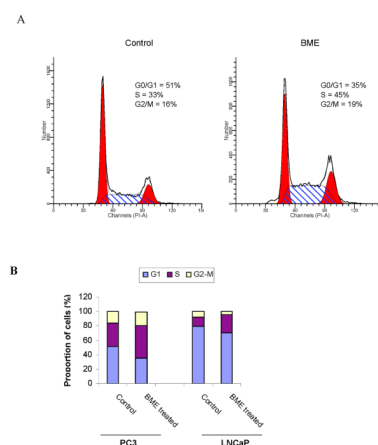
## REFERENCES

1. Jemal A, Siegel R, Ward E, Hao Y, Xu J, Thun MJ. Cancer statistic. *CA Cancer J Clin.* 2009; 59:225–249. [PubMed: 19474385]
2. Albertsen P. Predicting survival for men with clinically localized prostate cancer: what do we need in contemporary practice? *Cancer.* 2008; 112:1–3. [PubMed: 18000802]
3. So A, Gleave M, Hurtado-Col A, Nelson C. Mechanisms of the development of androgen independence in prostate cancer. *World J Urol.* 2005; 23:1–9. [PubMed: 15770516]
4. Surh YJ. Cancer chemoprevention with dietary phytochemicals. *Nat Rev Cancer.* 2003; 3:768–780. [PubMed: 14570043]
5. Grover JK, Yadav S, Vats V. Medicinal plants of India with anti-diabetic potential. *J Ethnopharmacol.* 2002; 81:81–100. [PubMed: 12020931]
6. Jayasooriya AP, Sakono M, Yukizaki C, Kawano M, Yamamoto K, Fukuda N. Effects of *Momordica charantia* powder on serum glucose levels and various lipid parameters in rats fed with cholesterol-free and cholesterol-enriched diets. *J Ethnopharmacol.* 2000; 72:331–336. [PubMed: 10967491]
7. Chao CY, Huang CJ. Bitter gourd (*Momordica charantia*) extract activates peroxisome proliferator-activated receptors and upregulates the expression of the acyl CoA oxidase gene in H4IIEC3 hepatoma cells. *J Biomed Sci.* 2003; 10:782–791. [PubMed: 14631118]
8. Chen Q, Chan LL, Li ET. Bitter melon (*Momordica charantia*) reduces adiposity, lowers serum insulin and normalizes glucose tolerance in rats fed a high fat diet. *J Nutr.* 2003; 133:1088–1093. [PubMed: 12672924]
9. Nerurkar PV, Lee YK, Motosue M, Adeli K, Nerurkar VR. *Momordica charantia* (bitter melon) reduces plasma apolipoprotein B-100 and increases hepatic insulin receptor substrate and phosphoinositide-3 kinase interactions. *Br J Nutr.* 2008; 100:751–759. [PubMed: 18321395]
10. Nerurkar PV, Lee YK, Nerurkar VR. *Momordica charantia* (bitter melon) inhibits primary human adipocyte differentiation by modulating adipogenic genes. *BMC Complement Altern Med.* 2010; 10:34. [PubMed: 20587058]

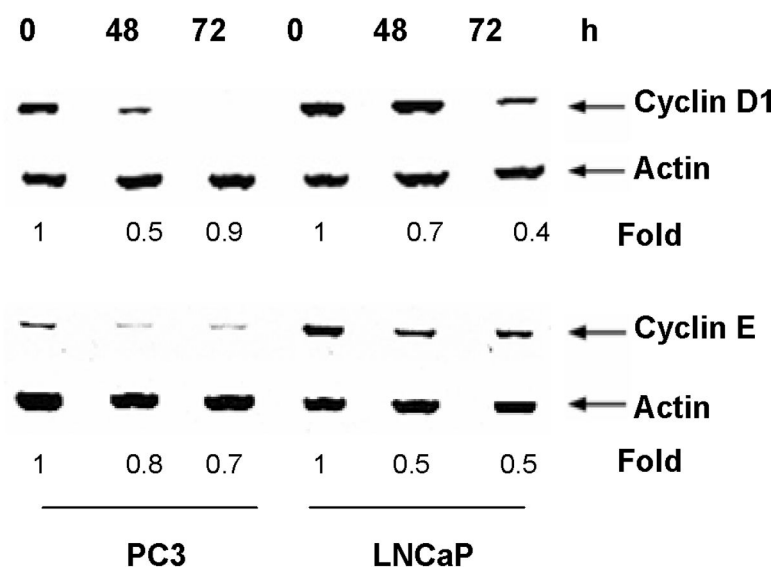
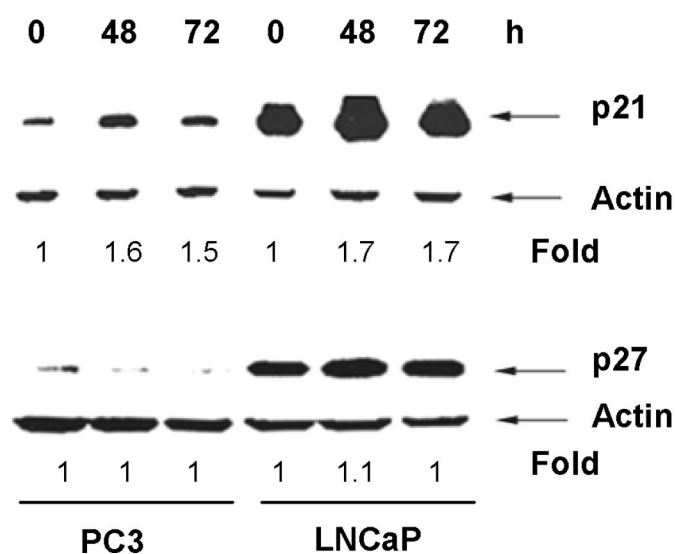
11. Nerurkar PV, Lee YK, Linden EH, Lim S, Pearson L, Frank J, et al. Lipid lowering effects of *Momordica charantia* (Bitter Melon) in HIV-1-protease inhibitor-treated human hepatoma cells, HepG2. *Br J Pharmacol*. 2006; 148:1156–1164. [PubMed: 16847441]
12. Jilka C, Striffler B, Fortner GW, Hays EF, Takemoto DJ. *In vivo* antitumor activity of the bitter melon (*Momordica charantia*). *Cancer Res*. 1983; 43:5151–5155. [PubMed: 6616452]
13. Lee-Huang S, Huang PL, Sun Y, Chen HC, Kung HF, Huang PL, et al. Inhibition of MDA-MB-231 human breast tumor xenografts and HER2 expression by anti-tumor agents GAP31 and MAP30. *Anticancer Res*. 2000; 20:653–659. [PubMed: 10810336]
14. Li M, Chen Y, Liu Z, Shen F, Bian X, Meng Y. Anti-tumor activity and immunological modification of ribosome-inactivating protein (RIP) from *Momordica charantia* by covalent attachment of polyethylene glycol. *Acta Biochim Biophys Sin (Shanghai)*. 2009; 41:792–799. [PubMed: 19727528]
15. Kohno H, Suzuki R, Noguchi R, Hosokawa M, Miyashita K, Tanaka T. Dietary conjugated linolenic acid inhibits azoxymethane-induced colonic aberrant crypt foci in rats. *Jpn J Cancer Res*. 2002; 93:133–142. [PubMed: 11856476]
16. Nagasawa H, Watanabe K, Inatomi H. Effects of bitter melon (*Momordica charantia* L.) or ginger rhizome (*Zingiber officinale* rosc) on spontaneous mammary tumorigenesis in SHN mice. *Am J Chin Med*. 2002; 30:195–205. [PubMed: 12230008]
17. Tsuzuki T, Tokuyama Y, Igarashi M, Miyazawa T. Tumor growth suppression by alpha-eleostearic acid, a linolenic acid isomer with a conjugated triene system, via lipid peroxidation. *Carcinogenesis*. 2004; 25:1417–1425. [PubMed: 14963014]
18. Ghosh AK, Steele R, Ray RB. c-myc Promoter-binding protein 1 (MBP-1) regulates prostate cancer cell growth by inhibiting MAPK pathway. *J Biol Chem*. 2005; 280:14325–14330. [PubMed: 15805119]
19. Ray RB, Raychoudhuri A, Steele R, Nerurkar P. Bitter melon (*Momordica charantia*) extract inhibits breast cancer cell proliferation by modulating cell cycle regulatory genes and promotes apoptosis. *Cancer Res*. 2010; 70:1925–1931. [PubMed: 20179194]
20. Gingrich JR, Barrios RJ, Kattan MW, Nahm HS, Finegold MJ, Greenberg NM. Androgen-independent prostate cancer progression in the TRAMP model. *Cancer Res*. 1997; 57:4687–4691. [PubMed: 9354422]
21. Klein RD, Kant JA. Opportunity knocks: the pathologist as laboratory genetics consultant. *Arch Pathol Lab Med*. 2006; 130:1603–1604. [PubMed: 17076520]
22. Gupta S, Hastak K, Ahmad N, Lewin JS, Mukhtar H. Inhibition of prostate carcinogenesis in TRAMP mice by oral infusion of green tea polyphenols. *Proc Natl Acad Sci U S A*. 2001; 98:10350–10355. [PubMed: 11504910]
23. Raina K, Singh RP, Agarwal R, Agarwal C. Oral grape seed extract inhibits prostate tumor growth and progression in TRAMP mice. *Cancer Res*. 2007; 67:5976–5982. [PubMed: 17575168]
24. Raina K, Blouin MJ, Singh RP, Majeed N, Deep G, Varghese L, et al. Dietary feeding of silibinin inhibits prostate tumor growth and progression in transgenic adenocarcinoma of the mouse prostate model. *Cancer Res*. 2007; 67:11083–11091. [PubMed: 18006855]
25. Singh SV, Warin R, Xiao D, Powolny AA, Stan SD, Arlotti JA, et al. Sulforaphane inhibits prostate carcinogenesis and pulmonary metastasis in TRAMP mice in association with increased cytotoxicity of natural killer cells. *Cancer Res*. 2009; 69:2117–2125. [PubMed: 19223537]
26. Shappell SB, Thomas GV, Roberts RL, Herbert R, Ittmann MM, Rubin MA, et al. Prostate pathology of genetically engineered mice: definitions and classification. The consensus report from the Bar Harbor meeting of the Mouse Models of Human Cancer Consortium Prostate Pathology Committee. *Cancer Res*. 2004; 64:2270–2305. [PubMed: 15026373]
27. Park KS, Ahn Y, Kim JA, Yun MS, Seong BL, Choi KY. Extracellular zinc stimulates ERK-dependent activation of p21(Cip/WAF1) and inhibits proliferation of colorectal cancer cells. *Br J Pharmacol*. 2002; 137:597–607. [PubMed: 12381673]
28. Wagner EF, Nebreda AR. Signal integration by JNK and p38 MAPK pathways in cancer development. *Nat Rev Cancer*. 2009; 9:537–549. [PubMed: 19629069]
29. Mukhopadhyay I, Sausville EA, Doroshow JH, Roy KK. Molecular mechanism of adaphostin-mediated G1 arrest in prostate cancer (PC-3) cells: signaling events mediated by hepatocyte



- growth factor receptor, c-Met, and p38 MAPK pathways. *J Biol Chem.* 2006; 281:37330–37344. [PubMed: 16956884]
30. Robertson BW, Bonsal L, Chellaiah MA. Regulation of Erk1/2 activation by osteopontin in PC3 human prostate cancer cells. *Mol Cancer.* 2010; 9:260. [PubMed: 20868520]
  31. Xia W, Spector S, Hardy L, Zhao S, Saluk A, Alemane L, et al. Tumor selective G2/M cell cycle arrest and apoptosis of epithelial and hematological malignancies by BBL22, a benzazepine. *Proc Natl Acad Sci U S A.* 2000; 97:7494–7499. [PubMed: 10861014]
  32. Greenberg NM, DeMayo F, Finegold MJ, Medina D, Tilley WD, Aspinall JO, et al. Prostate cancer in a transgenic mouse. *Proc Natl Acad Sci U S A.* 1995; 92:3439–3443. [PubMed: 7724580]
  33. Denmeade SR, Isaacs JT. Programmed Cell Death (Apoptosis) and Cancer Chemotherapy. *Cancer Control.* 1996; 3:303–309. [PubMed: 10765221]
  34. Kaur M, Agarwal C, Agarwal R. Anticancer and cancer chemopreventive potential of grape seed extract and other grape-based products. *J Nutr.* 2009; 139:1806S–1812S. [PubMed: 19640973]
  35. Khan N, Afaq F, Mukhtar H. Apoptosis by dietary factors: the suicide solution for delaying cancer growth. *Carcinogenesis.* 2007; 28:233–239. [PubMed: 17151090]
  36. Nerurkar P, Ray RB. Bitter melon: antagonist to cancer. *Pharm Res.* 2010; 27:1049–1053. [PubMed: 20198408]
  37. Zhu H, Zhang L, Wu S, Teraishi F, Davis JJ, Jacob D, et al. Induction of S-phase arrest and p21 overexpression by a small molecule 2[[3-(2,3-dichlorophenoxy)propyl] amino]ethanol in correlation with activation of ERK. *Oncogene.* 2004; 23:4984–4992. [PubMed: 15122344]
  38. Rahman KW, Li Y, Wang Z, Sarkar SH, Sarkar FH. Gene expression profiling revealed survivin as a target of 3,3'-diindolylmethane-induced cell growth inhibition and apoptosis in breast cancer cells. *Cancer Res.* 2006; 66:4952–4960. [PubMed: 16651453]
  39. Choi S, Kim TW, Singh SV. Ginsenoside Rh2-mediated G1 phase cell cycle arrest in human breast cancer cells is caused by p15 Ink4B and p27 Kip1-dependent inhibition of cyclin-dependent kinases. *Pharm Res.* 2009; 26:2280–2288. [PubMed: 19629651]
  40. Kobatake T, Yano M, Toyooka S, Tsukuda K, Dote H, Kikuchi T, Toyota M, et al. Aberrant methylation of p57KIP2 gene in lung and breast cancers and malignant mesotheliomas. *Oncol Rep.* 2004; 12:1087–1092. [PubMed: 15492797]
  41. Todd DE, Densham RM, Molton SA, Balmano K, Newson C, Weston CR, et al. ERK1/2 and p38 cooperate to induce a p21CIP1-dependent G1 cell cycle arrest. *Oncogene.* 2004; 23:3284–3295. [PubMed: 14981547]
  42. Edlund S, Bu S, Schuster N, Aspenström P, Heuchel R, Heldin NE, et al. Transforming growth factor-beta1 (TGF-beta)-induced apoptosis of prostate cancer cells involves Smad7-dependent activation of p38 by TGF-beta-activated kinase 1 and mitogen-activated protein kinase kinase 3. *Mol Biol Cell.* 2003; 14:529–544. [PubMed: 12589052]
  43. Sarfaraz S, Afaq F, Adhami VM, Malik A, Mukhtar H. Cannabinoid receptor agonist-induced apoptosis of human prostate cancer cells LNCaP proceeds through sustained activation of ERK1/2 leading to G1 cell cycle arrest. *J Biol Chem.* 2006; 281:39480–39491. [PubMed: 17068343]
  44. Moro L, Arbin AA, Marra E, Greco M. Constitutive activation of MAPK/ERK inhibits prostate cancer cell proliferation through upregulation of BRCA2. *Int J Oncol.* 2007; 30:217–224. [PubMed: 17143532]



**Fig 1. BME treatment in prostate cancer cells resulted in accumulation of cells at the S-phase**  
 Panel A. PC3 cells were treated with BME for 24 h, and stained with propidium iodide. DNA content was analyzed by flow cytometry. Results are represented as percent of cell population in G1, S and G2/M phases of the cell cycle. Panel B. Population of PC3 and LNCaP cells (%) at different cell cycle phased is shown by bar diagram. The experiments were repeated three times and representative data was presented.

**A****B**

**Fig. 2. Modulation of cell cycle regulatory proteins following BME treatment in prostate cancer cells**

PC3 and LNCaP cells were treated with BME at indicated time points and cell lysates were prepared for cell cycle molecules analysis. The expression of cyclin D1 and cyclin E (panel A), p21 and p27 (panel B) was examined by Western blot using specific antibodies. The blots were reprobbed with an antibody to actin for comparison of protein load. Densitometric scanning data after normalization with actin are shown at below of the bands.

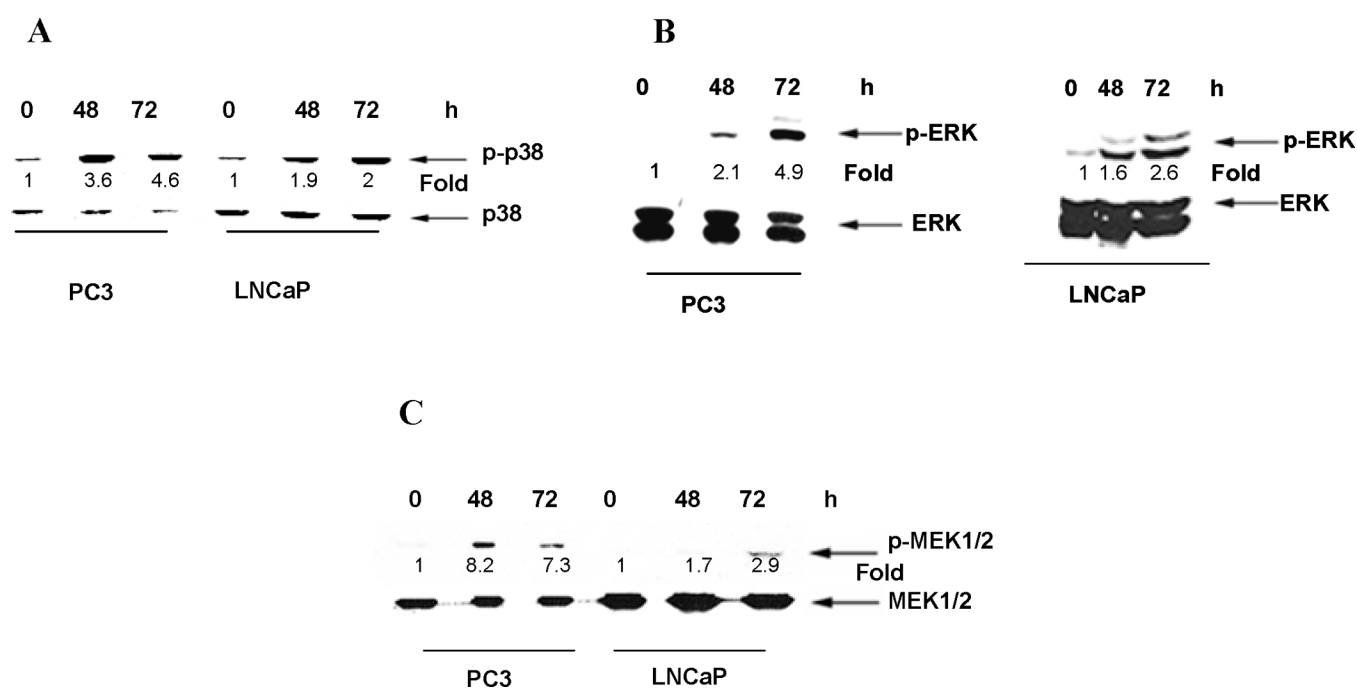


**Fig 3. BME treatment in prostate cancer cells activates p38, ERK 1/2 and MEK 1/2**

Cells were treated with BME at different time points. Cell lysates were analyzed for the expression of phospho-p38, p38 (panel A), phospho-ERK1/2 and ERK1/2 (panel B), phospho-MEK1/2 and MEK1/2 (panel C) by Western blot using specific antibodies. The blots were reprobbed with an antibody to actin for comparison of protein load. Densitometric scanning data after normalization with actin are shown at below of the bands.

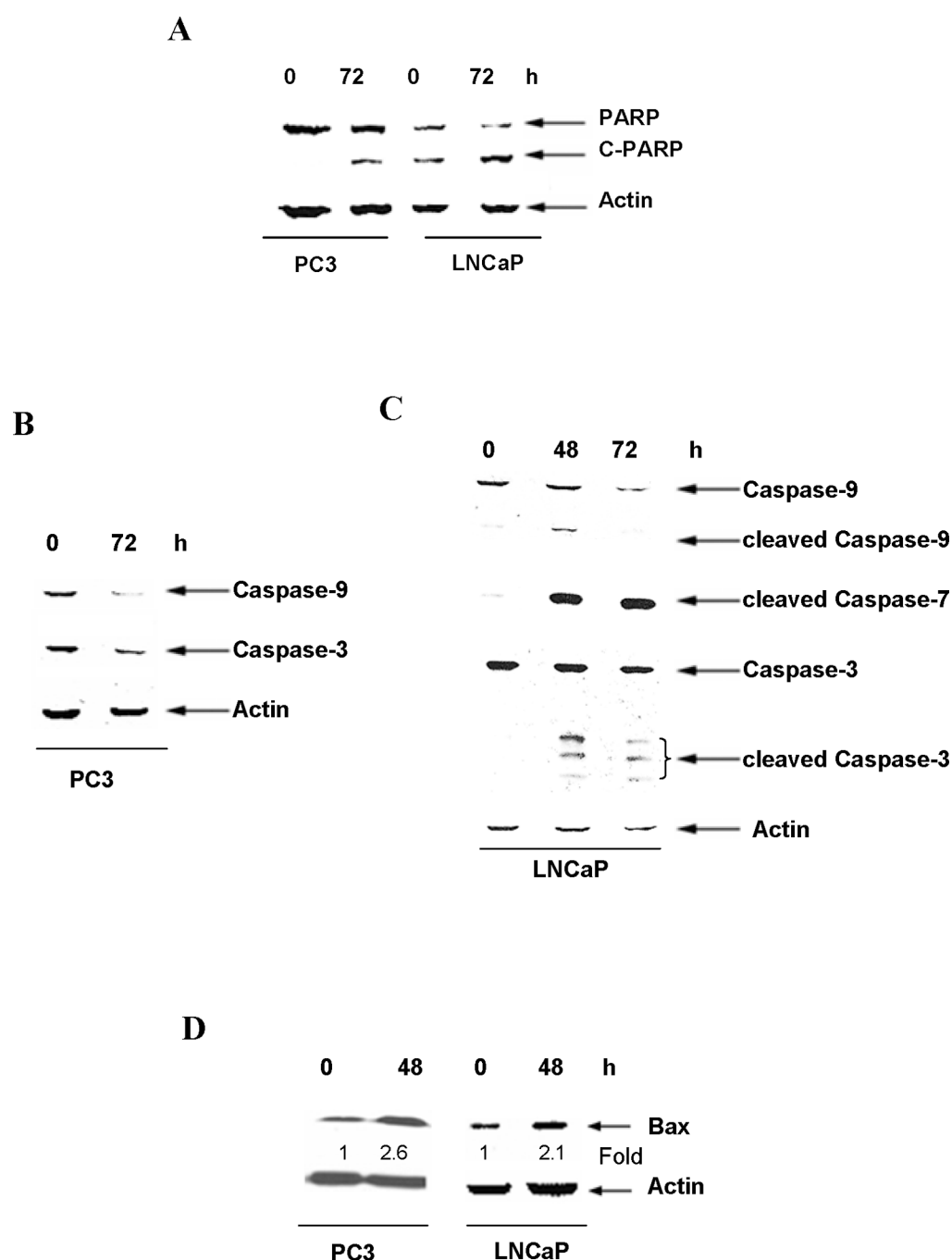


**Fig 4. BME mediated cell death involves PARP cleavage, caspase activation and increase Bax expression**

Lysates were prepared from PC3 and LNCaP cells treated or untreated with BME for 48 or 72 h, and subjected to Western blot analysis using a specific antibody to PARP or caspases. Following treatment of BME, PARP was cleaved to an 86 kD signature peptide (panel A). Treatment of PC3 cells (panel B) or LNCaP (panel C) with BME induces caspase 3/7 and 9. The antibody used in this experiment only recognized the cleaved caspase 7 form. Enhancement of Bax expression was observed in BME treated prostate cancer cells (panel D). The blot was reprobbed with an antibody to actin for comparison of equal protein load. Densitometric scanning data after normalization with actin are shown at below of the bands.



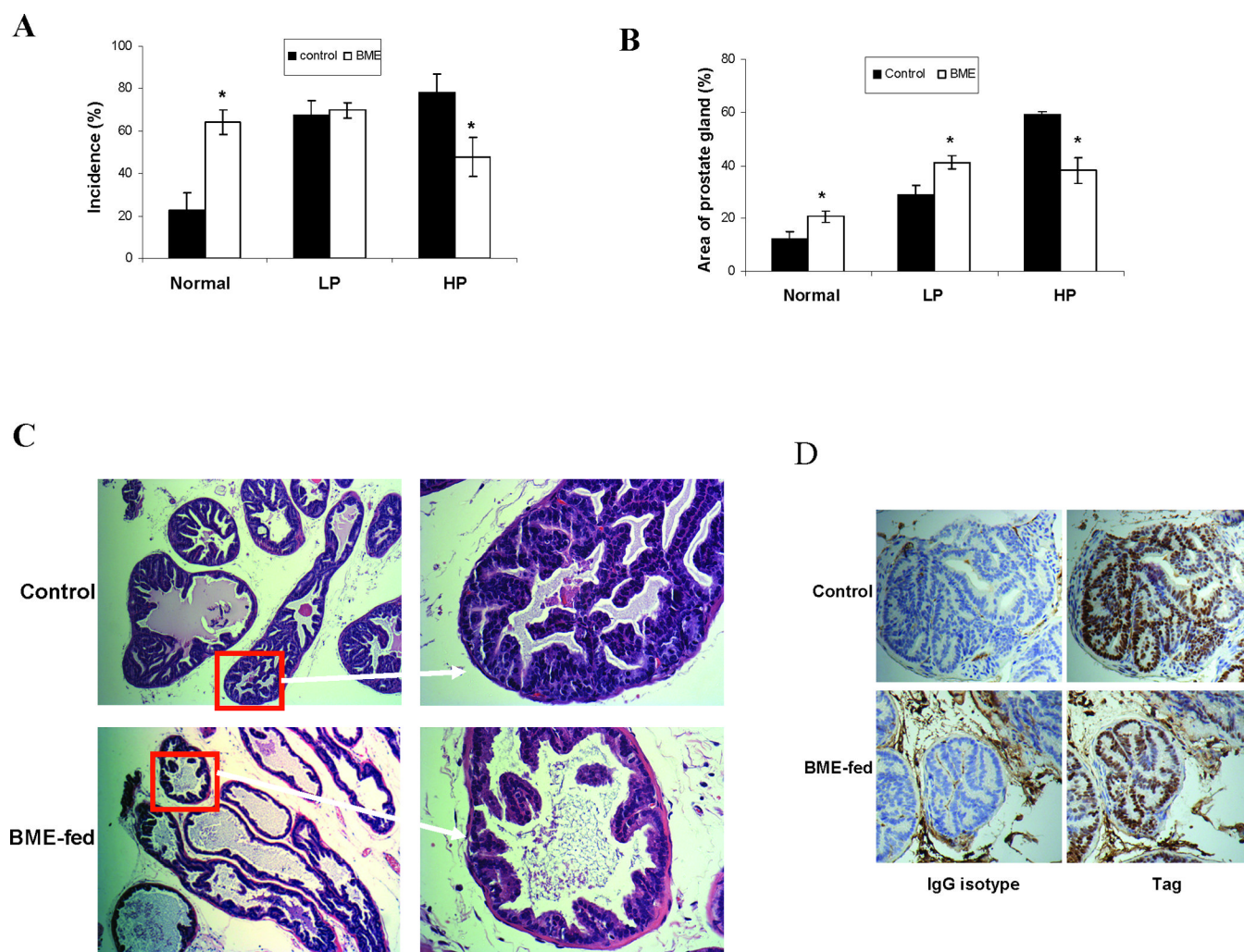
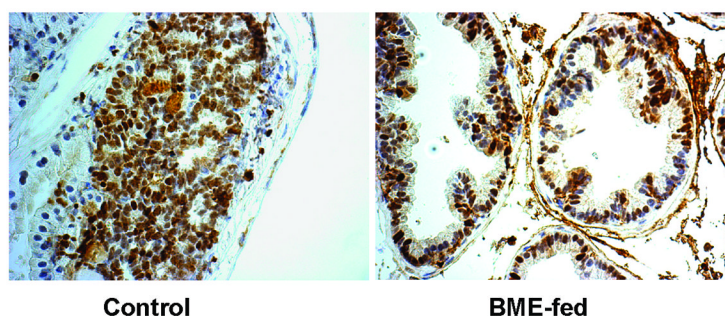


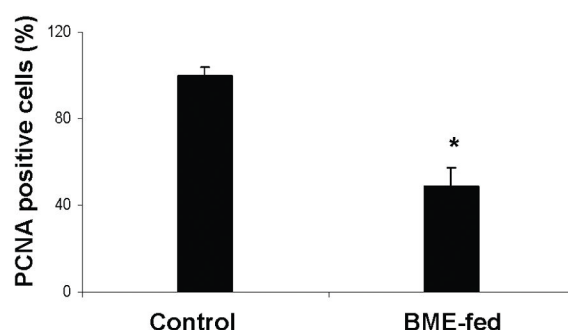
**Fig. 5. Oral BME administration in TRAMP mice delays prostate tumor progression**

Panel A. The incidence of histologic grades classified as normal prostate (N), low-grade PIN (LP), and high-grade-PIN (HP) in the DLP from control and BME-fed mice. Ten representative fields of each section of each mouse were scored for incidence of each histologic grade. The error bars represent variability of results in histologic grading between the two researchers (\* $P < 0.0002$ , 0.5 and 0.003, respectively). Panel B. The percentage of the area corresponding to the normal prostate, LP and HP in the DLP of control and BME-treated mice was scored by two researchers (\* $P < 0.002$ , 0.001 and 0.0001, respectively). Panel C. H&E staining of the DLP from control and BME-fed mice sacrificed at 21 weeks of age (magnification 100 $\times$ -left panels and 400 $\times$ -right panels). Panel D. SV40 T-antigen expression in a representative DLP of a control and BME-fed TRAMP mouse (magnification, 200 $\times$ ).

A



B



C



D

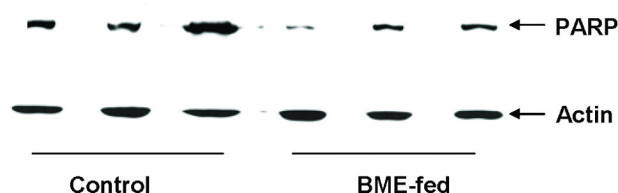


**Fig 6. BME feeding in TRAMP mice inhibits cell proliferation *in vivo***

Panel A. The immunohistochemical staining for PCNA in representative DLP of a control and BME-fed TRAMP mouse (magnification, 200 $\times$ ) are shown. Panel B. Quantification of PCNA-positive cells for determination of proliferation index (\* $P < 0.0015$ ). Panel C. Western blot of PCNA in prostate tissues isolated from both control and BME fed groups TRAMP mice. The blot was reprobbed with an antibody to actin for comparison of protein load. Panel D. Western blot analysis displayed PARP expression in prostate tissues isolated from BME fed group as compared to control TRAMP mice. The blot was reprobbed with an antibody to actin for comparison of protein load.